DMD #22640

The Application of Molecular Modeling for Prediction of Substrate Specificity

in Cytochrome P450 1A2 Mutants

Youbin Tu, Rahul Deshmukh[1], Meena Sivaneri and Grazyna D. Szklarz

Department of Basic Pharmaceutical Sciences, School of Pharmacy, West Virginia

University, Morgantown, WV 26506

Running Title: Predicting substrate specificity of P450 1A2 mutants

Corresponding Author: Grazyna D. Szklarz

Department of Basic Pharmaceutical Sciences, School of Pharmacy, West Virginia University, P.O. Box 9530, Morgantown, WV 26506-9530.

Tel. (304) 293-1473

Fax: (304) 293-2576

E-mail: gszklarz@hsc.wvu.edu

Manuscript Information:

text pages:	40
number of tables:	4
number of figures:	5
number of references:	32
Abstract:	222 words
Introduction	542 words
Discussion	1338 words

Abbreviations:

P450, cytochrome P450; WT, wild type; NADPH, β-nicotinamide adenine dinucleotide phosphate reduced form; ES, enzyme-substrate complex

DMD #22640

ABSTRACT:

Molecular dynamics (MD) simulations of 7-ethoxy and 7-methoxyresorufin bound in the active site of P450 1A2 wild type and various mutants were used to predict changes in substrate specificity of the mutants. A total of 26 multiple mutants representing all possible combinations of five key amino acid residues which are different between P450 1A1 and 1A2, were examined. The resorufin substrates were docked in the active site of each enzyme in the productive binding orientation and MD simulations were performed on the ES complex. Ensembles collected from MD trajectories were then scored based on geometric parameters relating substrate position with respect to the activated oxoheme cofactor. The results showed a high correlation between the previous experimental data on P450 1A2 wild type and single mutants with respect to the ratio between 7-ethoxyresorufin-*O*-deethylase (EROD) and 7-methoxyresorufin-*O*-demethylase (MROD) activities, and the equivalent *in silico* E/M scores. Moreover, this correlation served to establish linear regression models utilized to evaluate E/M scores of multiple P450 1A2 mutants. Seven mutants, all of them incorporating the L382V substitution, were predicted to shift specificity to that of P450 1A1. The predictions were then verified experimentally. The appropriate P450 1A2 multiple mutants were constructed by site-directed mutagenesis, expressed in *E. coli*, and assayed for EROD and MROD activities. Out of six mutants, five demonstrated increased EROD/MROD ratio confirming modeling predictions.

Cytochromes P450 constitute a large family of heme-thiolate monooxygenase enzymes widely found in nature (Nelson et al, 1996). These enzymes are capable of catalyzing the oxidation of a wide variety of both xenobiotic and endogenous compounds. However, even closely related isoforms may exhibit different catalytic activities.

Human P450 1A1 and 1A2, the two major isoforms in P450 1A subfamily, share 72% amino acid sequence identity but display different substrate specificities. P450 1A1 prefers to metabolize benzo[a]pyrene and other polycyclic aromatic hydrocarbons (PAHs), while P450 1A2 favors the oxidation of heterocyclic and aromatic amines (Guengerich, 2005; Kawajiri and Hayashi, 1996). Likewise, they also exhibit different substrate specificities with resorufin substrates like 7-ethoxyresorufin and 7-methoxyresorufin (Nerurkar et al., 1993; Burke et al., 1994). Therefore, the P450 1A1/1A2 system provides a good model for exploring the basis for functional differences between individual P450 enzymes.

The experimentally determined structure of a protein can provide valuable insight into its function. Homology modeling is an alternative method to obtain the structure when the crystal structure is not available (Szklarz et al., 2000). Molecular dynamics (MD) simulations on the enzyme-substrate complex could provide information on whether the substrate is sterically accessible for oxidation, which could be used for predicting the activities of different isoforms. Indeed, this type of approach has been applied to predict the catalytic activities, coupling/uncoupling efficiency and substrate specificity of several bacterial and eukaryotic P450s and their mutants (Paulsen et al., 1996; Harris and Loew, 1995; Kuhn et al., 2001). Likewise, using a homology model of P450 1A1 (Szklarz and Paulsen, 2000), we have successfully employed MD simulations on the enzyme-substrate

complex to evaluate the productive binding orientations of benzo[a]pyrene and fatty acids (Ericksen and Szklarz, 2005).   This application not only rationalized the metabolite profiles of several P450 1A1 substrates but also indicated that steric influence could be quantitatively evaluated using the MD-based steric scoring approach.

Docking of resorufin substrates in the active site of the homology model of P450 1A1 suggested that residue Val-382 may play an important role in binding and *O*-dealkylation of these substrates (Szklarz and Paulsen, 2002).   This was confirmed experimentally in further studies with P450 1A1 V382L and V382A mutants (Liu et al., 2003).   We have also examined the function of five key residues that are different between P450 1A1 and 1A2, and thus may affect enzyme specificity (Liu et al., 2004).   Indeed, residue replacement resulted in different levels of specificity changes in reciprocal P450 1A1 and 1A2 single mutants, as indicated by the ratio of 7-methoxyresorufin-*O*-dealkylation (MROD) to 7-ethoxyresorufin-*O*-dealkylation (EROD) (EROD/MROD ratio).   However, no single reciprocal mutation was capable of entirely conferring the activities of one isoform onto another, and only residue substitutions at position 382 in both P450 1A1 and 1A2 led to the shift in specificity.

The objective of the present study was to investigate whether any multiple mutations in P450 1A2 may convert the resorufin specificity characteristic of P450 1A2 to that of 1A1. A total of 26 multiple mutants representing all possible combinations of five key amino acid residues which are different between P450 1A1 and 1A2, were evaluated using molecular modeling methods, such as molecular dynamics, and modeling predictions were verified experimentally.   This type of approach may help in the determination of P450 specificity.

Materials and Methods

Materials. The DNA sequencing and mutagenic oligonucleotide primers were synthesized at the Sigma Genosys (Woodlands, Texas). QuickChange site-directed mutagenesis toolkit and StrataPrep plasmid miniprep kit were purchased from Stratagene (La Jolla, CA). *E. coli* DH5α competent cells were obtained from Invitrogen Corporation (Carlsbad, CA). 7-Methoxyresorufin, 7-ethoxyresorufin, resorufin, NADPH, ampicillin, isopropyl-β-D-thiogalactopyranoside (IPTG), δ-aminolevulinic acid (ALA), 3-[(3-cholamidopropyl) dimethylammonio]-1-propanesulfonate (CHAPS), dilauroyl-L-3-phosphatidyl choline (DLPC) and phenylmethanesulfonyl fluoride (PMSF) were from Sigma (St. Louis, MO). Ni-NTA Agarose and gel extraction kit were purchased from Qiagen (Valencia, CA). All other chemicals used were of analytical grade and were obtained from standard commercial sources.

Construction of Multiple Mutants of P450 1A2. The clones of P450 1A1 WT, P450 1A2 WT and 1A2 single mutants, T124S, T223N, V227G, N312L and L382V, were constructed previously (Liu et al., 2003; 2004). Double to quintuple P450 1A2 multiple mutants were created using pCWori+ plasmids containing the His-tag P450 1A2 WT or its single mutants cDNA as templates (Liu et al, 2004). QuickChange® Site-Directed Mutagenesis Kit was used, and mutagenic primers were the same as utilized previously for the construction of single P450 1A2 mutants (Liu et al., 2004). A typical protocol described in the QuikChange® mutagenesis instruction manual was used with minor modifications. The PCR conditions were adjusted as follows: 1 cycle at 95°C for 1-2 min,

6

DMD #22640

followed by 20-25 cycles of temperature cycling – denaturing at 95°C for 30 sec, annealing at

55-65°C for 40-60 sec, followed by extension at 72°C for an additional minute.   The

cycling was followed with a final extension at 72°C for 10 min.   The PCR product was then

treated with restriction enzyme *Dpn* I to digest the parental DNA template.   Post-digestion

product containing the mutated plasmid with nicked circular strands was transformed into XL

1-B supercompetent cells.   The plasmid containing the mutant DNA was purified using

Qiagen® plasmid purification kit.   The double mutants were constructed by adding an

additional mutation to the single mutants and the triple mutants were constructed in a similar

fashion from the double mutants.   The mutations in the plasmids were verified by nucleotide

sequence analysis carried out at the Molecular Genetics Instrumentation Facility, University

of Georgia (Athens, GA).

Protein Expression and Purification.   The His-tag-containing P450 1A1 and 1A2

WT and 1A2 mutants were expressed in *E. coli* DH5α cells and purified as previously

described (Liu et al., 2004), except that during the purification of P450 1A2 WT and mutants,

0.5 M KCl was added to the solubilization buffer.   The final purity of the enzymes was

assessed by SDS-PAGE.   Western blots were performed using anti-human P450 1A1/1A2

(Oxford Biomedical, Oxford, MI) and P450 proteins were visualized as described (Kedzie et

al., 1991).   P450 content was determined by reduced CO/reduced difference spectra (Omura

and Sato, 1964) and protein was measured by the method of using Folin phenol reagent

(Lowry et al., 1951).

P450 Activity Assays.   7-Methoxy- and 7-ethoxyresorufin *O*-dealkylase activities of P450 1A1 WT, 1A2 WT and their mutants were assayed as described previously at 37ºC by fluorometric detection of resorufin, using excitation and emission wavelengths of 550 nm and 585 nm, respectively (Liu et al., 2003; 2004).   The reaction mixture contained 50 nM P450, 100 nM P450 reductase and 10 μM substrate in a 0.1 M potassium phosphate buffer, and the reaction was initiated by the addition of 10 µl of 100 mM NADPH, as described (Liu et al., 2003; 2004).   Rat cytochrome P450 reductase was expressed in *E. coli* and purified as described (Liu et al., 2003; 2004).   The formation of resorufin was detected as the increase of fluorescence intensity against time.   The reaction rate was quantified with resorufin standards.   All measurements were performed in triplicate.

Molecular Modeling Methods: General.   Molecular modeling was performed on an SGI Octane workstation using the InsightII software (Accelrys, San Diego, CA). The homology model of P450 1A2 have been constructed previously (Liu et al., 2004).   The crystal structure of P450 1A2 (pdb code: 2hi4.pdb) was obtained courtesy of Dr. Eric F. Johnson, The Scripps Research Institute, La Jolla, CA (Sansen et al., 2007).   Minimization and molecular dynamics (MD) simulations were performed using the Discover module of InsightII, with the consistent valence force field (CVFF) supplemented with parameters for heme and ferryl oxygen (Paulsen and Ornstein, 1991; 1992).   Trajectory data were extracted using the Analysis module of InsightII and graphed with Origin 8 (Northampton, MA).

DMD #22640

MD Simulations with P450 1A2 WT and Mutants. The structures of P450 1A2 mutants were obtained by the replacement of selected amino acids in the homology model of P450 1A2 followed by 500 iterations of energy minimization using steepest descent gradient, essentially as described earlier (Liu at al., 2003; 2004). 7-Methoxy- and 7-ethoxyresorufins were previously docked into the active site of P450 1A2 using the Affinity module of InsightII (Liu et al., 2004). These enzyme-alkoxyresorufin complexes served as the starting point for the subsequent dynamic docking phase which refined the position of the substrate in the productive binding orientation.

Dynamic docking involved 5 ps constrained MD simulations at 300 K. During that period, only the substrate and protein residues within 15 Å from the substrate were allowed to move. The non-bond interaction cutoff was set at 15 Å, a residue-based non-bond list cutoff was 16 Å, and the distance dependent dielectric was used. The distance between the ferryl oxygen and one of the hydrogens to be abstracted was restrained to 2.75-3.25 Å with a restoring force ($k = 100$ kcal·mol^{-1}·Å^{-2}) applied to keep the oxidation site close to the ferryl oxygen. Another distance restraint of 4.10-4.35 Å between the carbon atom at the oxidation site and the ferryl oxygen (C$^{...}$O) was applied concurrently to keep the angle (C–H$^{...}$O) as close as possible to linear (Kuhn et al., 2001).

In the second part of MD simulations, all the restraints were abolished and the substrate was allowed to move freely for the subsequent 50 ps. Simulation conditions were exactly as described above.

Sampling and Scoring of Productive Binding Orientation.   The coordinates of each enzyme-substrate complex were saved every 250 fs giving the total of 120 MD frames obtained following the initial 10 ps of dynamic docking.   All trajectories were examined with the Analysis module of InsightII.   To score the likelihood of hydroxylation, each sampled frame of a given enzyme-substrate complex was evaluated using different sets of geometric criteria.

The productive orientation of the substrate is usually defined by two parameters: 1) the distance, r, between the hydrogen atom at the oxidation site of the substrate, and the ferryl oxygen atom (H$\cdots$O distance), and 2) the angle, θ, between the ferryl oxygen, hydrogen atom to be abstracted, and the carbon at the oxidation site (C–H$\cdots$O angle).   Since the linear transition state is assumed for hydrogen abstraction to occur, ideally, the distance should be close to 3 Å and the angle is postulated to be 180° (Fig. 1A).

In this work, we used four types of criteria to define an effective score or "hit".   Criterion P defined a hit as a frame in which the distance r was equal to or smaller than 3 Å (r $\leq$ 3.0 Å), while criterion PM combined the condition on distance r with the condition on angle θ, required to be larger than 135° ($r \leq 3.0$ Å and $\theta \geq 135°$).   Less stringent criterion Q required the distance r not to exceed 3.5 Å, and criterion QN added the requirement on angle not to exceed 120° ($r \leq 3.5$ Å and $\theta \geq 120°$).   An example of such an evaluation is shown in Fig. 1C and D, where criterion QN is used to assess hits, represented by frames located within the grey region.

This procedure was applied to all single and multiple mutants complexed with either 7-ethoxy- or 7-methoxyresorufin.   The "E/M score" representing *in silico* specificity was

DMD #22640

defined as the ratio of hits obtained with 7-ethoxyresorufin to those obtained with

7-methoxyresorufin.

Prediction of Substrate Specificity of P450 1A2 Multiple Mutants.   The E/M scores

obtained for single mutants were used to construct a linear regression model that linked these

results with experimental specificity expressed as the EROD/MROD ratio defined previously

(Liu et al., 2004).   The best correlation between the two was seen for criterion P, with R^2

equal to 0.9612 (p < 0.001), and for criterion QN, where $R^2 = 0.9097$ (p < 0.001).

Therefore, these two criteria were used for prediction of specificity in multiple 1A2 mutants.

The specific equations were as follows:

for criterion P:

Predicted Specificity = 0.3900 (±0.0658) + 0.0138 (±0.0014) x E/M score

and for criterion QN:

Predicted Specificity = 0.2961 (±0.1093) + 0.1470 (±0.0231) x E/M score

Predicted specificity was expressed as predicted EROD/MROD ratio.

Comparisons with the Crystal Structure of P450 1A2.   The homology model of

P450 1A2 has been compared with the recently available crystal structure of this enzyme

(Sansen et al., 2007).   The RMSD between the crystal and the model has been measured by

superimposing the backbones of the two structures using different regions as a basis.   These

included: a) overall structure, b) the active site region, and c) the previously mentioned five

11

key residues only.   The active site was defined as a region containing residues within 10 Å

from docked 7-ethoxyrersorufin, and key residues were T124, T223, V227, N312 and L382.

7-Ethoxyresorufin and 7-methoxyresorufin were placed in the crystal structure of P450

1A2 WT in positions similar to those in the homology model.   MD simulations of

enzyme-substrate complexes were performed in the same way as with the homology model

and the results were analyzed as described above, by counting hits using different geometrical

criteria.

Results

Substrate Mobility in the Active Site of P450 1A2 WT and Single Mutants. Our previous studies with P450 1A1 and 1A2 reciprocal active site mutants demonstrated that the replacement of a single residue may affect the specificity of alkoxyresorufin metabolism (Liu et al., 2004). In particular, mutations at position 382 in both P450 1A1 and 1A2 shifted substrate specificity from one enzyme to another. However, none of the single residue substitutions at positions 124, 223, 227 and 312 (location in the 1A2 sequence) completely interconverted P450 1A1 and 1A2 specificities (Liu et al., 2004). Therefore, the goal of our present studies was to identify multiple mutants in which the specificity of one enzyme was fully conferred to another.

In the first part of this project, we used molecular modeling methods, in particular molecular dynamics (MD), to make predictions concerning the results of multiple residue substitutions in P450 1A2. Initially, P450 1A2 WT and its five single mutants, which were investigated earlier (Liu et al., 2004), were selected as the training set for MD simulations in order to provide information regarding specificity prediction.

Molecular dynamics simulations were used both as a part of the docking strategy to refine the substrate orientation in the active site, and as a means to predict the product profile, similar to our previous work (Ericksen and Szklarz, 2005). Thus, following the energy minimization, the first 5 ps of restrained MD served to optimally place an alkoxyresorufin in a productive binding orientation. Figure 2A shows the resulting orientation of 7-methoxy- and 7-ethoxyresorufin in the active site of P450 1A2, with five key residues, T124, T223, V227, N312 and L382, displayed.

DMD #22640

The productive binding orientation has been defined by two geometric parameters, r and θ, as illustrated in Fig. 1A (see also Materials and Methods). During 5 ps of dynamic docking, the distance, r, between the ferryl oxygen of the heme and the hydrogen atom of the substrate to be abstracted was restrained to ~ 3.0 Å and remained fairly constant (see Fig. 1B). In contrast, the angle, θ, between the ferryl oxygen, hydrogen atom to be abstracted, and the carbon at the oxidation site, alternated between 120° and 180° (Fig. 1B).

The transition from the restrained state to the free moving state was achieved over 5 ps. For each enzyme-substrate complex, 120 frames from unrestrained MD (productive phase) were then collected starting at 10 ps time point. In most cases, after removing the restraints, the substrate moved rapidly into another, more stable orientation where it remained throughout the remainder of the simulation. This led to sudden and radical changes in relevant distances and angles, followed by a reasonably steady phase of equilibrium, as illustrated in Fig. 1B.

A detailed analysis of the geometrical parameters was performed for each snapshot of every enzyme-substrate complex to evaluate the tendency of the ligand to remain in the productive binding orientation during the productive dynamic phase. Each enzyme-substrate complex displayed a unique characteristic MD "fingerprint" regarding the distances and angles related to the productive binding orientation. Two examples are shown in Fig. 1C and D. For instance, for the P450 L382V mutant, both hydrogens at the oxidation site of 7-ethoxyresorufin remained at about 3 Å from the ferryl oxygen, while all hydrogens of 7-methoxyresorufin were much farther away (Fig. 1D), in agreement with our earlier

findings (Liu et al., 2004). Overall, in this mutant, 7-ethoxyresorufin showed a greater

preference to occupy a productive binding orientation than 7-methoxyresorufin.

Specificity of 7-Methoxy and 7-Ethoxyresorufin Oxidation by P450 1A2 Single Mutants. In our previous work (Liu et al., 2004) we expressed the specificity of various

P450 1A1 and 1A2 mutants in terms of the ratio of 7-ethoxyresorufin *O*-deethylation to

7-methoxyresorufin *O*-demethylation (EROD/MROD ratio). This approach allowed us to

successfully evaluate alterations in activity upon residue substitution and the degree to which

the activity of one enzyme was conferred upon another. Therefore, we also used the

EROD/MROD ratio as a measure of enzyme specificity in the present work.

Essentially, the EROD/MROD ratio was expressed in terms of its *in silico* equivalent,

the E/M score, which represented the number of "hits" for 7-ethoxyresorufin divided by the

number of "hits" for 7-methoxyresorufin. The "hits", i.e., the number of conformers with

the substrate occupying the productive binding orientation, were derived from the analysis of

the productive phase of MD simulations using four sets of different criteria with respect to

distance r and angle θ. Criteria P ($r \leq 3.0$ Å) and PM ($r \leq 3.0$ Å and $\theta \geq 135°$) were more

stringent than criteria Q ($r \leq 3.5$ Å) and QN ($r \leq 3.5$ Å and $\theta \geq 120°$), and criteria PM and QN

included the conditions on both distance and angle (see Materials and Methods).

Table 1 shows the number of hits for the two substrates and the resulting E/M scores for

various P450 1A2 single mutants. Depending upon the set of criteria used in counting hits,

the E/M scores may vary widely. Usually the hit was a positive integer with very few

exceptions when no hits were found, such as for the 7-methoxyresorufin–P450 1A2 N312L

complex.   For most mutants, E/M scores were low and similar to the scores obtained for the

WT 1A2, which correlated well with experimental specificity.   In contrast, the score

obtained for the 1A2 L382V mutant was much higher, as was the corresponding

EROD/MROD ratio, consistent with our previous findings (Liu et al., 2004).   This general

agreement between the *in silico* scores and experimental results allowed us to construct linear

regression models.   As shown in Fig. 3, the specificities of single 1A2 mutants as predicted

by the models were very close to the experimental ones, confirming good correlations.

Therefore, the models were subsequently used to predict EROD/MROD ratios for multiple

mutants, as detailed in Materials and Methods.

Specificity of 7-Methoxy and 7-Ethoxyresorufin Oxidation by P450 1A2 Multiple

Mutants.   In order to determine which multiple substitutions of five key residues in P450

1A2 could potentially lead to the shift in specificity towards that of P450 1A1 WT, we

performed MD simulations with all possible multiple mutants.   Figure 4 shows the

schematic tree structure of all possible combinations of mutations containing one substitution,

namely Leu-382→Val.   The number of mutants with this particular amino acid replacement,

varying from double to quintuple, was fifteen, and, when this procedure was repeated for all

five key residues, the total number of all possible mutants, excluding repeated combinations,

rose to twenty six.   The MD simulations were performed with all these mutants using

exactly the same protocol as applied in the case of P450 1A2 WT and single mutants (see

Materials and Methods).   The results were then evaluated using criteria P, PM, Q and QN,

as described for the single mutants.

The E/M scores were used to classify the mutants with respect to the possibility of a significant shift in substrate specificity. The *in silico* descriptor of P450 1A2 L382V, a mutant known to display a considerable shift in specificity, served as a reference to select likely multiple mutant candidates. As shown in Table 2, seven out of 26 mutants had E/M scores equal to or above 80% of that for the L382V mutant, and were thus predicted to display a similarly high shift in specificity. Furthermore, these predictions were upheld with all four geometric criteria. The mutants under consideration were T124S-L382V, T223N-L382V, V227G-L382V, T124S-T223N-L382V, T124S-N312L-L382V, T223N-N312L-L382V and N312L-L382V. Thus, all the multiple mutants predicted to significantly alter specificity had to include the substitution of Leu-382→Val, which further confirms the exceptional role of this residue in producing specificity shifts from P450 1A2 to 1A1 and vice versa, with alkoxyresorufin substrates (Liu et al., 2004). Interestingly, the quintuple mutant, T124S-T223N-V227G-N312L-L382V, was not predicted to display altered specificity.

The MD-derived E/M scores were used to calculate the values of EROD/MROD ratios for selected 1A2 multiple mutants based on two linear regression models constructed for the single mutants (see the previous section). The extrapolated ratios then served as a basis for the comparison with the experimental values.

Experimental Validation of Modeling Predictions. By employing modeling, we have significantly reduced the number of P450 1A2 multiple mutants, from twenty six to seven, needed for further experimental studies. Six out of seven multiple mutants have been

successfully created by site-directed mutagenesis and were active in biochemical assays following purification. The double mutant V227G-L382V has not been successfully expressed; its expression level was very low and the protein was unstable.

Overall, mutant enzymes differed in expression levels and activities, as also noted previously (Liu et al., 2004). For example, P450 content of purified preparations varied from ~1 to 60 nmol/ml, and specific content was from 0.2 to 60 nmol P450/mg protein, with holoenzyme in the range of 1-32% (data not shown). Table 3 shows the activities and EROD/MROD ratios for various multiple mutants. Due to a considerable variability in the levels of activities, the EROD/MROD ratio is the best discriminator among the mutants, in agreement with our previous findings (Liu et al., 2004). It should be noted that the EROD/MROD ratios for the P450 1A2 WT and the L382V mutant were 0.32 and 2.27, respectively (Table 3), displaying a slight difference when compared to the previous values of 0.4 and 2.0 (Table 1, Liu et al., 2004).

Figure 5 shows a comparison between the predicted and experimental EROD/MROD ratios for the selected P450 1A2 multiple mutants. As mentioned above, the predicted specificities were extrapolated from two linear regression models, which established a correlation between *in silico* E/M scores and experimental EROD/MROD ratios using P450 1A2 WT and its five single mutants (see Materials and Methods). Five out of six multiple 1A2 mutants have demonstrated the expected high shift in specificities from P450 1A2 towards 1A1, with the exception of the double mutant, T124S-L382V (see also Table 3). Moreover, the linear model using criterion P ($r \leq 3.0$ Å) seemed to give much closer predictions than that using criterion QN ($r \leq 3.5$ Å and $\theta \geq 120^{\circ}$). In the case of the latter,

the predicted specificity values (EROD/MROD ratios) were all much higher than the experimental ratios (data not shown). The comparison between the experimental and predicted specificity using criterion P for the selected P450 1A2 multiple mutants is shown in Fig. 5. Interestingly, in the case of the double mutant T124S-L382V, both prediction models have yielded much higher specificity (criterion P: 1.8; QN: 3.6) than its experimental value of 0.34. The experimental EROD/MROD ratio for this mutant was thus comparable to that of the P450 1A2 WT (Table 3).

Comparison of the Homology Model of P450 1A2 with the Crystal Structure. At the final stage of this project, the crystal structure of human P450 1A2 has been solved, with the resolution of 1.95Å (Sansen et al., 2007). Thus, it became necessary to compare the homology model of P450 1A2 with the crystal structure in order to validate our current study.

With respect to the overall structure, the homology model resembles closely its structural template, P450 2C5. This could be the inevitable drawback of the homology modeling methodology itself. The overall RMSD between the model and the P450 1A2 crystal was 4.4 Å when all residues (i.e., residues 34-513) were included in the superimposition. This seemingly large value is not that surprising, since this type of comparison includes both structurally conserved regions (SCRs) and non-SCR segments, especially loops on the protein surface, which are usually created in a random fashion with a lot of variability. Consequently, it would be much more reasonable to compare directly the core regions containing most of the SCRs, which are directly involved in the interactions with substrates; in this case, the RMSD value is reduced to 3.5 Å. Structural comparisons were

further performed using additional functional sets as the criteria, including active site residues

and the five key residues currently under investigation.   The environment formed by only

the five key residues and that produced by all active site residues (i.e., residues within 10 Å

of 7-ethoxyresorufin docked in the crystal structure) had a similar structural divergence of

~2.5 Å and 2.6 Å, respectively, much lower than a corresponding value for the global protein

structure.   This indicates that the active site containing the five key residues is well

constructed in the homology model and comparable with the crystal structure, as shown in

Fig. 2B.   Moreover, in either option of superimposition, i.e., when only key residues or all

active site residues were superimposed, all of the five key residues except N312 display

reasonably good structural similarity, as indicated by small values of backbone RMSD, which

were as follows: for T124 - 1.1 and 1.92 Å, respectively; for T223 - 2.4 and 2.22 Å; for V227

– 1.44 and 1.68 Å; for N312 – 3.92 and 4.09 Å; and for L382 – 2.11 and 1.53 Å (Fig. 2B).

Therefore, N312 may not be properly positioned in the homology model, which might have

resulted in artificially high and extremely variable E/M scores observed earlier with the

single mutant P450 1A2 N312L (see Table 1).

The dynamic behavior of substrates bound in the active site of the crystal structure has

been also investigated using the protocol established for the homology model.   As shown in

Table 4, regardless of the criteria used, the number of hits for 7-methoxyresorufin was

significantly higher than for 7-ethoxyresorufin, in full agreement with experimental data.

However, the E/M scores are similar in both the model and the crystal only in the case of

criterion QN ($r \leq 3.5$ Å and $\theta \geq 120^{o}$).   This may indicate the inaccuracy of the homology

model and/or the specific conditions applied in the computer simulation and data analysis.

Discussion

In the current work, we used molecular modeling methods to predict the changes in specificity of P450 1A2 toward alkoxyresorufin substrates upon introducing multiple residue substitutions simultaneously in the active site. The objective was two-fold: to determine which residue combinations could completely interconvert the specificity from P450 1A2 to 1A1, and to develop a fast computational method for prediction of substrate specificity. Among twenty six possible multiple mutants, ranging from double to quintuple, the molecular dynamics-based scoring method predicted seven of them to shift specificity. Five predictions were further confirmed experimentally by site-directed mutagenesis and biochemical assays.

These studies follow our previous work concerning the importance of five active site residues that are different between P450 1A1 and 1A2 (Liu et al., 2004). Based on those findings, only mutations at position 382 shifted specificity from one enzyme to another using alkoxyresorufins as substrates. Similarly, our present results indicate that all mutations that likewise affect specificity contain a substitution at this position (Table 2). The only exception was the quintuple mutant, T124S-T223N-V227G-N312L-L382V, which, contrary to expectations, was not predicted to display altered specificity. Moreover, no multiple P450 1A2 mutant exhibited substrate specificity characteristic of P450 1A1. This further strengthens the idea that the specificity is not simply determined by a linear combination of these five substitutions, but other residues, outside of the active site, must be taken into account. Similar conclusions were reported in earlier studies with single mutants of other related isoforms, such as P450 2B1 and 2B2 (He et al., 1994), and 2B4 and 2B5 (Szklarz et

al., 1996).   Moreover, in the P450 2B4 and 2B5 system, multiple active site mutations were not sufficient to fully interconvert activities (He et al., 1996), analogous to our studies.

In the case of P450 1A1 and 1A2, a number of residues have been identified by others as important for activity.   However, in most cases, the residues studied were different than those we investigated here and in earlier work (Liu et al., 2003; 2004).   For example, more recently, Kim and Guengerich (2004) reported that a triple mutant, E163-V193M-K170Q, was five times faster than the wild type 1A2 in 7-methoxyresorufin O-demethylation.   These residues, however, are located far from the active site.   Lately, a combinatorial approach has been applied by Taly et al. (2007) to discriminate between 1A1 and 1A2 using alkoxyresorufin substrates.   However, the residues we identified as important (Liu et al,, 2003; 2004) were not confirmed by this study, possibly due to exclusion of this region of the sequence.   In a very recent study, Lewis and colleagues (2007) described the construction of a homology model of P450 1A1 based on the structure of P450 1A2, and confirmed the importance of residues 124, 227 and 382 (numbers in 1A2) for binding of 7-ethoxyresorufin. Moreover, Met-121 (Leu-123 in 1A2) was also suggested to have some contributions in binding of this substrate (Lewis et al., 2007).

A comparison of our homology model with the recently crystallized structure of P450 1A2 (Sansen et al., 2007) showed that the active site exhibits reasonably good structural resemblance (Fig. 2B).   The placement of the four studied residues, T124, T223, V227 and L382 is very similar; in contrast, the position of N312 appears to be significantly shifted in the model.   The latter phenomenon is likely responsible for poor correlations between computational and experimental data concerning the N312L mutant (see Table 1), and might

have affected molecular modeling results with other mutants.   In the case of P450 2D6, the

crystallization of this enzyme helped to explain various mutagenesis data, often confirming

the conclusions drawn from previous homology models (Rowland et al., 2006).   For

example, Asp-301 was implicated in catalytic activity as early as 1993, based on an early

model of the active site region of P450 2D6 (Koymans et al., 1993), and Glu-216 was also

suggested to play a role in substrate binding (Lewis et al., 1997).   In general, most 2D6

models correctly located key residues, with some exceptions, such as residues Phe-481 and

Phe-483 (de Groot et al., 1999).   On the other hand, the latter discrepancy may reflect

protein motion, and can be resolved by molecular dynamic simulations (Rowland et al.,

2006).

In some respects, the current work is also a continuation of our previous studies on

regiospecificity of P450 1A1-mediated oxidations (Ericksen and Szklarz, 2005), where

modeling methodology was successfully applied to rationalize product profiles observed with

several 1A1 substrates.   This earlier approach has been expanded so that we not only used

computational methodology for predictions concerning the specificity of alkoxyresorufin

oxidation, but also verified them experimentally.   As observed with P450 1A1 oxidations,

steric effects also seem to be of major importance in the case of alkoxyresorufin oxidations

by P450 1A2.   In this approach, we neglected substrate electronic considerations, but,

nevertheless, electronic factors can also provide contributions.   For example, they may

account for differences in the number of hits observed for a given enzyme with

7-methoxyresorufin as a substrate versus the number of hits seen with 7-ethoxyresorufin

(Table 1).   However, the E/M score can serve as a basis for the comparison among different enzymes, and used as a descriptor to correlate with experimental specificity.

The predictive power of this computationally-derived model is affected by the length of the simulation and the number of samples collected for analysis.   In our case, after the minimization of the E-S complex, we applied restraints to force the oxidation site of the substrate close to the ferryl oxygen, and then removed them to evaluate the stability of the productive binding orientation.   This approach has been effectively utilized in our previous work (Ericksen and Szklarz, 2005).   Molecular dynamics with distance restraints has also been successfully applied to investigate the metabolism of sirolimus by P450 3A4 (Kuhn et al., 2001).   This, we believe, circumvents the need for long simulations and gives this approach a potential to be routinely used as a rapid method to predict specificity and/or product profile.

An important factor in molecular modeling when using homology models is the accuracy of such a model, which depends to a large extent on the template used (Szklarz et al., 2000).   In that respect, the 1A2 model used in these studies, based on the structure of P450 2C5, can be expected to differ from the crystal structure of P450 1A2.   As discussed above, the active site structure of this homology model was quite similar to that of the crystal. Consequently, new models of highly related enzymes, such as P450 1A1, should now be based on the crystal structure of P450 1A2.   As reported recently, a new 1A1 model was superior to the previous ones (Lewis et al., 2007).

However, the question of structural "correctness" is not an easy one.   Proteins display structural flexibility, and in the case of P450s, this is confirmed by the existence of multiple

structures for the same isoform, that may display various degrees of structural differences, often dependent upon the ligand bound (Poulos, 2003; 2005).   Thus, the basic P450 fold is very flexible, which is further supported by molecular dynamics simulations that can "map the route" from one structure to another.   For example, in the case of P450 BM-3, MD simulations showed that binding of substrate may induce conformational shift leading to a structurally distinct P450-ligand complex (Chang and Loew, 1999).   A recent review by Hammes-Schiffer and Benkovic (2006) examines the link between protein conformational motion and enzyme catalysis, and presents evidence for a network of coupled motions throughout the protein fold that facilitate chemical reactions.   Thus, thermal motions of the enzyme, substrate, and cofactor lead to conformational sampling of configurations that provide favorable environment for catalysis.   Therefore, we should take into account P450 flexibility and reexamine the value of MD simulations.

The current work has successfully combined MD-based computational predictions with their experimental verification, and the majority of predictions concerning changes in substrate specificity in P450 1A2 multiple mutants were confirmed.   This technique may thus provide a prototype for rapid evaluation of the catalytic properties of different P450 isoforms, and its application to the crystal structures should further enhance its accuracy.

DMD #22640

and Molecular Modeling Laboratory, Department of Basic Pharmaceutical Sciences, School

of Pharmacy, West Virginia University, Morgantown, WV.

References

Burke MD, Thompson S, Weaver RJ, Wolf CR and Mayer RT (1994) Cytochrome P450 specificities of alkoxyresorufin O-dealkylation in human and rat liver. *Biochem Pharmacol* **48:**923-936.

Chang Y-T and Loew GH (1999) Molecular dynamic simulations of P450 BM3 – examination of substrate-induced conformational change. *J Biomol Struct Dyn* **16:** 1189-1203.

de Groot MJ, Ackland MJ, Horne VA, Alexander AX and Jones BC (1999) Novel Approach To Predicting P450-Mediated Drug Metabolism: Development of a Combined Protein and Pharmacophore Model for CYP2D6. *J Med Chem* **42:**1515 -1524.

Ericksen SS and Szklarz GD (2005) Regiospecificity of human cytochrome P450 1A1-mediated oxidations: the role of steric effects. *J Biomol Struct Dyn* **23**: 243-256.

Guengerich FP (2005) Human cytochrome P450 enzymes, in *Cytochrome P450: Structure, Mechanism and Biochemistry,* 3rd edition (Ortiz de Montellano PR ed) pp 377-530, Kluwer Academic/Plenum Publishers, New York.

Hammes-Schiffer S and Benkovic SJ (2006) Relating protein motion to catalysis. *Annu Rev Biochem* **75:** 519-541.

Harris D and Loew GL (1995) Prediction of regiospecific hydroxylation of camphor analogs by cytochrome P450cam. *J Am Chem Soc* **117**:2738-2746.

He YQ, Luo ZS, Klekotka PA, Burnett VL and Halpert JR (1994) Structural determinants of cytochrome P450 2B1 specificity: Evidence for five substrate recognition sites. *Biochemistry* **33**:152-160.

He YQ, Szklarz GD and Halpert JR (1996) Interconversion of the androstenedione hydroxylase specificities of cytochromes P450 2B4 and 2B5 upon simultaneous site-directed mutagenesis of four key substrate recognition residues. *Arch Biochem Biophys* **335**:152-160.

Kawajiri K and Hayashi S-i (1996) The CYP1 family, in *Cytochromes P450: Metabolic and Toxicological Aspects* (Ioannides C ed) pp 77-97, CRC Press, Boca Raton.

Kim D and Guengerich FP (2004) Enhancement of 7-methoxyresorufin O-demethylation activity of human cytochrome P450 1A2 by molecular breeding. *Arch Biochem Biophys* **432**:102-108.

Koymans LM, Vermeulen NP, Baarslag A and Donné-Op den Kelder GM (1993) A preliminary 3D model for cytochrome P450 2D6 constructed by homology model building. *J Comput-Aided Mol Des* **7:**281-289.

Kuhn B, Jacobsen W, Christians U, Benet LZ, and Kollman PA (2001) Metabolism of sirolimus and its derivative everolimus by cytochrome P450 3A4: Insights from docking, molecular dynamics, and quantum chemical calculations. *J Med Chem* **44**: 2027-2034.

Lewis DF, Eddershaw PJ, Goldfarb PS and Tarbit MH (1997) Molecular modelling of cytochrome P4502D6 (CYP2D6) based on an alignment with CYP102: structural studies on specific CYP2D6 substrate metabolism. *Xenobiotica* **27:**319-39.

Lewis BC, Mackenzie PI and Miners JO (2007) Comparative homology modeling of human cytochrome P450 1A1 (CYP1A1) and confirmation of residues involved in

DMD #22640

7-ethoxyresorufin O-deethylation by site-directed mutagenesis and enzyme kinetic analysis. *Arch Biochem Biophys* 468: 58-69.

Liu J, Ericksen SS, Besspiata D, Fisher CW, Szklarz GD (2003) Characterization of substrate binding to cytochrome P450 1A1 using molecular modeling and kinetic analyses: case of residue 382. *Drug Metab Dispos* **31**: 412-420.

Liu J, Ericksen SS, Besspiata D, Fisher CW, Szklarz GD (2004) The effect of reciprocal active site mutations in human cytochromes P450 1A1 and 1A2 on alkoxyresorufin metabolism. *Arch Biochem Biophys* **424**: 33-43.

Lowry OH, Rosebrough NJ, Farr AL, Randall RJ (1951) Protein measurement with the Folin phenol reagent. *J Biol Chem* **193:** 265-75.

Nelson DR, Koymans L, Kamataki T, Stegeman JJ, Feyereisen R, Waxman DJ, Waterman MR, Gotoh O, Coon MJ, Estabrook RW, Gunsalus IC and Nebert DW (1996) P450 superfamily: update on new sequences, gene mapping, accession numbers and nomenclature. *Pharmacogenetics* **6**: 1-42.

Nerurkar PV, Park SS, Thomas PE, Nims RW and Lubet RA (1993) Methoxyresorufin and benzyloxyresorufin: substrates preferentially metabolized by cytochromes P450 1A2 and 2B, respectively, in the rat and mouse. *Biochem Pharmacol* **46**: 933-943.

Omura T and Sato R (1964) The carbon monoxide-binding pigment of liver microsomes. *J Biol Chem* **239**:2379–2387.

Paulsen MD and Ornstein RL (1991) A 175 psec molecular dynamics simulation of camphorbound cytochrome P-450cam. *Proteins* **11**: 184–204.

Paulsen MD and Ornstein RL (1992) Predicting the product specificity and coupling of cytochrome P450cam. *J Comput-Aided Mol Des* **6**: 449–460.

Paulsen MD, Manchester JI and Ornstein RL (1996) Using molecular modeling and molecular dynamics simulation to predict P450 oxidation products. *Methods Enzymol* **272**: 347-357.

Poulos TL (2003) Cytochrome P450 flexibility. *Proc Natl Acad Sci USA* **100:** 13121-13122.

Poulos TL (2005) Structural and functional diversity in heme monooxygenases. *Drug Metab Disp* **33:** 10-18.

Rowland P, Blaney FE, Smyth MG, Jones JJ, Leydon VR, Oxbrow AK, Lewis CJ, Tennant MG, Modi S, Eggleston DS, Chenery RJ and Bridges AM (2006) Crystal structure of human cytochrome P450 2D6. *J Biol Chem* **281:** 7614-7622.

Sansen S, Yano JK, Reynald R, Schoch GA, Griffin KJ, Stout CD and Johnson EF (2007) Adaptations for the oxidation of polycyclic aromatic hydrocarbons exhibited by the structure of human P450 1A2. *J Biol Chem* **282**: 14348-14355.

Szklarz GD, He YQ, Kedzie KM, Halpert JR and Burnett VL (1996) Elucidation of amino acid residues critical for unique activities of rabbit cytochrome P450 2B5 using hybrid enzymes and reciprocal site-directed mutagenesis with rabbit cytochrome P450 2B4. *Arch Biochem Biophys* **327**: 308-318.

Szklarz GD, Graham SE and Paulsen MD (2000) Molecular modeling of mammalian cytochromes P450: application to study enzyme function. *Vitam and Horm* **58**: 53-86.

Szklarz GD and Paulsen MD (2002) Molecular modeling of cytochrome P450 1A1: enzyme-substrate interactions and substrate binding affinities. *J Biomol Struct Dyn* **20**: 155-162.

Taly V, Urban P, Truan G and Pompon D (2007) A combinatorial approach to substrate discrimination in the P450 CYP1A subfamily. *Biochim Biophys Acta* **1170:** 446-457.

DMD #22640

Footnotes

[1]Current address: GPRD, Drug Metabolism, Abbott Park, Abbott, IL 60064

DMD #22640

Legends for Figures

FIGURE 1.   A scheme for MD-based scoring of productive binding orientations with 7-ethoxyresorufin as a substrate using a geometric criterion QN ($r \leq 3.5$ Å and $\theta \geq 120^{o}$). A: Productive binding orientation of 7-ethoxyresorufin showing the two geometric parameters, r and θ. r is the distance between the hydrogen to be abstracted and the ferryl oxygen; θ is the angle between ferryl oxygen, hydrogen atom to be abstracted, and the carbon at the oxidation site.   B: Plots of r and θ for hydrogens of the substrate that may be abstracted over 55 ps of MD trajectory in P450 1A2 WT. H_1 of 7-ethoxyresorufin is blue and H_2 is red; grey regions indicate where criterion QN is satisfied with respect to distance r and angle θ.   C: Ensemble of substrate orientations described by r and θ, sampled from 120 frames after 10 ps MD simulations in P450 1A2 WT.   The top panel represents 7-ethoxyresorufin (H_1: red, H_2: blue) and the bottom one is 7-methoxyresorufin (H_1: red, H_2: blue, H_3: green).   The grey region indicates where the geometric criterion QN is satisfied.   D: Similar plots as in C, except that the enzyme is P450 1A2 L382V.

FIGURE 2.   The active site of P450 1A2.   A: 7-Ethoxyresorufin (green) and 7-methoxyresorufin (orange) docked in the productive binding orientation in the active site of the P450 1A2 WT homology model.   Five key residues have been displayed in blue as sticks, with their Cα shown as CPK.   Heme is shown in red.   B: The comparison of the homology model and the crystal structure of P450 1A2.   The two structures have been superimposed using the backbones of the active site (10 Å around 7-ethoxyresorufin) as a

33

basis. The homology model is blue and the crystal structure is magenta. The five key residues in the crystal structure are brown.

FIGURE 3. Experimental and predicted specificity for P450 1A2 WT and five single mutants. The specificity was expressed as EROD/MROD ratio. Two linear regression models were used to calculate predicted specificity: predicted specificity 1 was based on criterion P ($r \leq 3.0$ Å), while predicted specificity 2 was based on criterion QN ($r \leq 3.5$ Å and $\theta \geq 120^{\circ}$).

FIGURE 4. The schematic tree structure of possible combinations of mutations containing a L382V substitution. A total of 15 multiple mutants: 4 double, 6 triple, 4 quadruple and 1 quintuple mutant, is possible in this case. Similar trees were constructed for other mutations. After removing repeated combinations, this gave a total of 26 multiple mutants containing all possible mutations of the five key residues.

FIGURE 5. Experimental and predicted specificity for the selected multiple mutants of P450 1A2. The specificity was expressed as EROD/MROD ratio. The linear regression model used to calculate predicted specificity was based on criterion P ($r \leq 3.0$ Å).

DMD #22640

TABLE 1

Geometric analysis of the molecular dynamics results for the wild type and five single

mutants of P450 1A2.

Enzyme type		Criterion P[a]	Criterion PM	Criterion Q	Criterion QN	Experimental Specificity
1A2 WT	No. of Hits:					
	EOR	32	0	89	8	
	MOR	21	7	67	33	
	E/M score	**1.52**	0	1.33	**0.24**	0.4
T124S	No. of Hits:					
	EOR	29	2	89	7	
	MOR	15	0	59	4	
	E/M score	**1.93**	2[b]	1.51	**1.75**	0.6
T223N	No. of Hits:					
	EOR	21	0	59	4	
	MOR	21	6	77	24	
	E/M score	**1**	0	0.77	**0.17**	0.4
V227G	No. of Hits:					
	EOR	22	3	85	5	
	MOR	29	6	100	16	
	E/M score	**0.76**	0.5	0.85	**0.31**	0.4
N312L	No. of Hits:					
	EOR	23	1	89	4	
	MOR	0	0	0	0	
	E/M score	**23**[b]	1[b]	89[b]	**4**[b]	0.5
L382V	No. of Hits:					
	EOR	114	6	212	32	
	MOR	1	0	5	3	
	E/M score	**114**	6[b]	42.4	**10.7**	2.0

Hits represent the MD frames were the substrate, 7-ethoxyresorufin (EOR) or 7-methoxyresorufin (MOR), was in the productive binding orientation, as evaluated by various criteria.   E/M score is the ratio of hits for EOR to those for MOR.

[a]Criterion P: $r \leq 3.0$ Å; PM: $r \leq 3.0$ Å & $\theta \geq 135°$; Q: $r \leq 3.5$ Å; QN: $r \leq 3.5$ Å & $\theta \geq 120°$. The details are in Materials and Methods.

[b]One hit was assigned to the denominator to replace 0.

Boldface represents the scores used to construct a linear regression model.   The details are described in Materials and Methods.

TABLE 2

In silico *E/M scores for the P450 1A2 multiple mutants.*

Enzyme type	E/M score (Criterion P)	E/M score (Criterion PM)	E/M score (Criterion Q)	E/M score (Criterion QN)
T124S-L382V	**105**	**11**	**45.3**	**23**
T223N-L382V	**93**	**10**	**183**	**51**
V227G-L382V	**92**	**22**	**40.8**	**31.5**
T124S-T223N-L382V	**102**	**14**	**60.7**	**56**
T124S- V227G -L382V	39.5	30	18.6	19
T124S- T223N -L382V	100	14	31	21.7
T124S-T223N-V227G-L382V	79	24	150	58
T124S-N312L-L382V	**101**	**9**	**37.2**	**38**
T223N-N312L-L382V	**109**	**10**	**38.4**	**45**
V227G-N312L-L382V	86	18	37.5	64
T124S-T223N-N312L-L382V	1	0	0.57	0
T124S-V227G-N312L-L382V	66	28	26	77
T223N-V227G-N312L-L382V	71	15	29	19.3
T124S-T223N-V227G-N312L-L382V	0	0	0.33	0
N312L-L382V	**112**	**9**	**63.7**	**37**
T124S-N312L	32	0	40	7
T124S-T223N-N312L	27	0	7.8	1.86
T124S-T223N-V227G-N312L	55	20	17.3	8.8
T124S-V227G-N312L	17.7	10.5	9.72	5.38
T223N-N312L	0	0	0	0
T223N-V227G-N312L	9	0	4	0.2
V227G-N312L	31	1	28	14
T124S-T223N	0.9	0.3	1.02	0.24
T124S-V227G	3.14	3.5	4.92	3.86
T223N-V227G	12	2.33	8.4	4.83

DMD #22640

T124S-T223N-V227G	7	4	14	8
L382V*	**114**	**6**	**42.4**	**10.7**

*L382V is used as a reference. The multiple mutants predicted to display large shifts in specificity are shown in **boldface.** All selected mutants demonstrated an E/M score that was 80% or more of that for L382V. See Results for details.

TABLE 3

Alkoxyresorufin O-dealkylase activities of P450 1A2 WT, the L382V mutant and multiple 1A2

mutants predicted to display large shifts in specificity.

P450 1A2	Activity		% WT Activity		EROD/MROD
	EROD[a]	MROD[b]	EROD	MROD	Ratio
WT	2.6[c]	8.04	100	100	0.32
L382V	0.68	0.3	26.1	3.73	2.27
T124S-L382V	0.12	0.35	4.61	4.35	0.34
T223N-L382V	0.57	0.43	21.9	5.35	1.32
T124S-T223N-L382V	0.19	0.09	7.31	1.12	2.11
T124S-N312L-L382V	4.05	2.75	156	34.2	1.47
T223N-N312L-L382V	5.1	2.4	196	29.9	2.13
N312L-L382V	1.76	0.71	67.7	8.83	2.48

[a] 7-Methoxyresorufin *O*-demethylase activity

[b] 7-Ethoxyresorufin *O*-deethylase activity

[c] *O*-dealkylase activity as *nmol product min^{-1} nmol P450^{-1}*. The experimental variability

(SD) was within 10%.

TABLE 4

Geometric analysis of the molecular dynamics results for the wild type P450 1A2 using either

the homology model or the crystal structure

Enzyme type		Criterion P	Criterion PM	Criterion Q	Criterion QN	Experimental Specificity
	No. of Hits:					
1A2 WT	EOR	32	0	89	8	
(Homology)	MOR	21	7	67	33	
	E/M score	1.52	0	1.33	0.24	0.4
	No. of Hits:					
1A2 WT	EOR	0	0	27	26	
(Crystal)	MOR	137	10	211	49	
	E/M score	0	0	0.13	0.53	0.4

Hits represent the MD frames where the substrate, 7-ethoxyresorufin (EOR) or 7-methoxyresorufin (MOR), was in the productive binding orientation, as evaluated by various criteria. E/M score is the ratio of hits for EOR to those for MOR.

[a]Criterion P: $r \leq 3.0$ Å; PM: $r \leq 3.0$ Å & $\theta \geq 135°$; Q: $r \leq 3.5$ Å; QN: $r \leq 3.5$ Å & $\theta \geq 120°$. The details are in Materials and Methods.

[b]One hit was assigned to the denominator to replace 0.

Figure 1
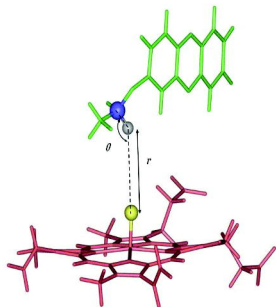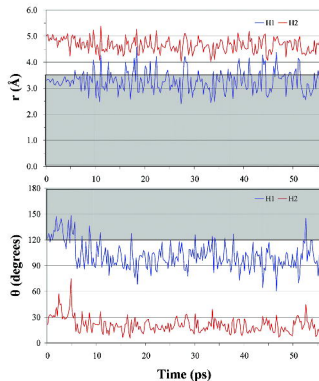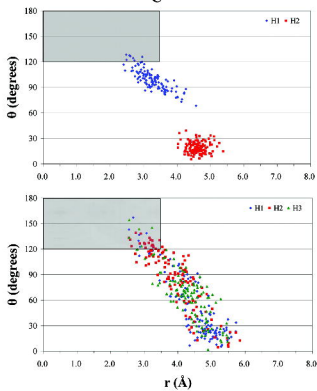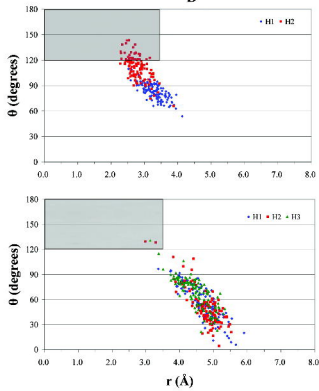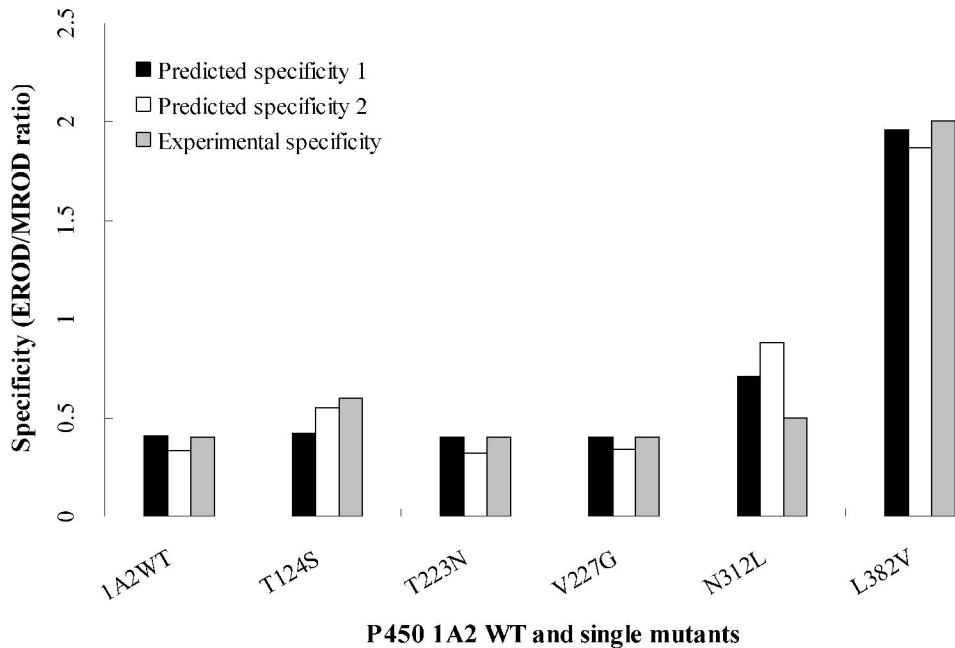
Figure 2
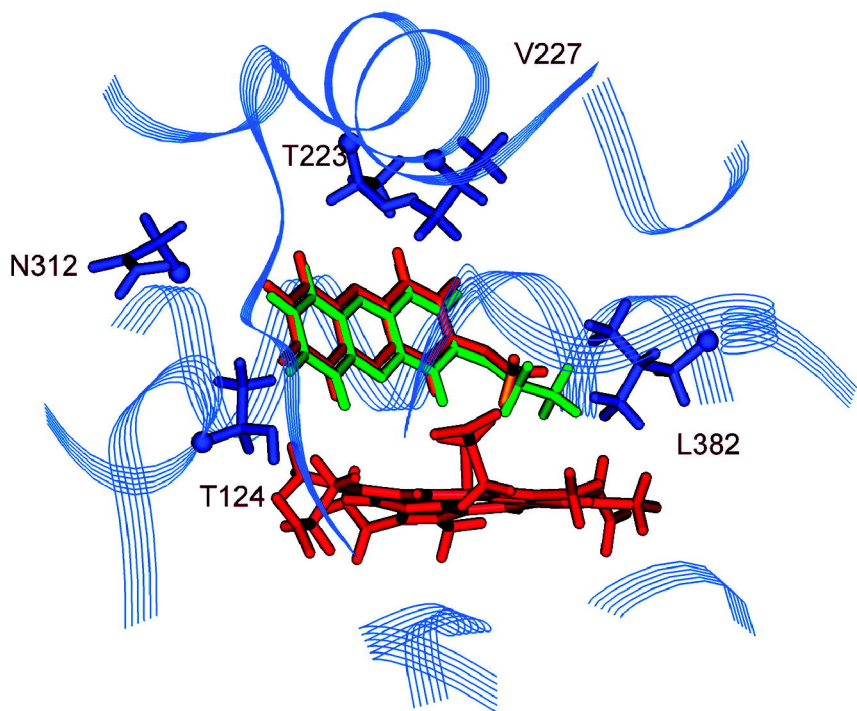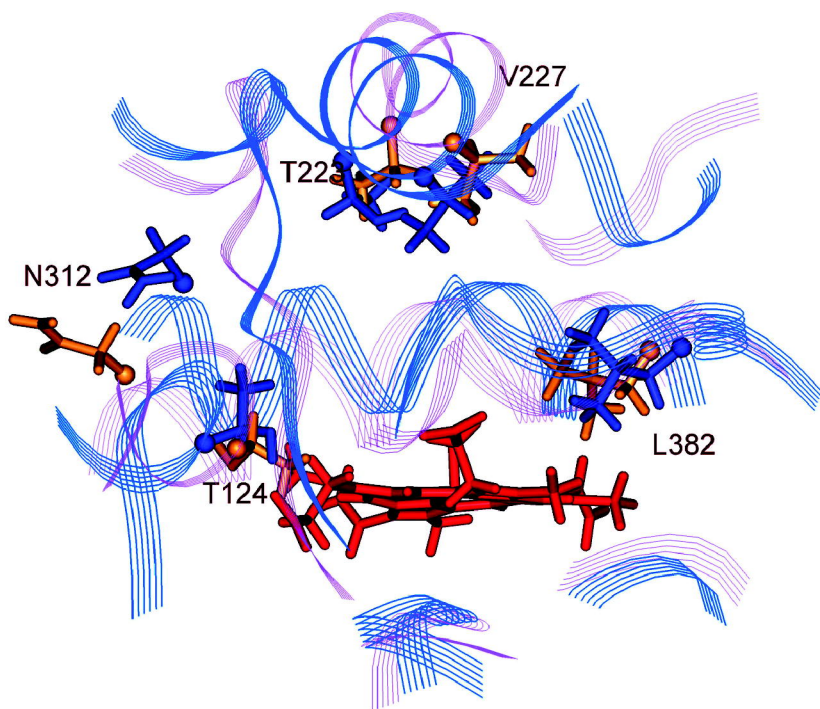
Figure 3

Figure 4
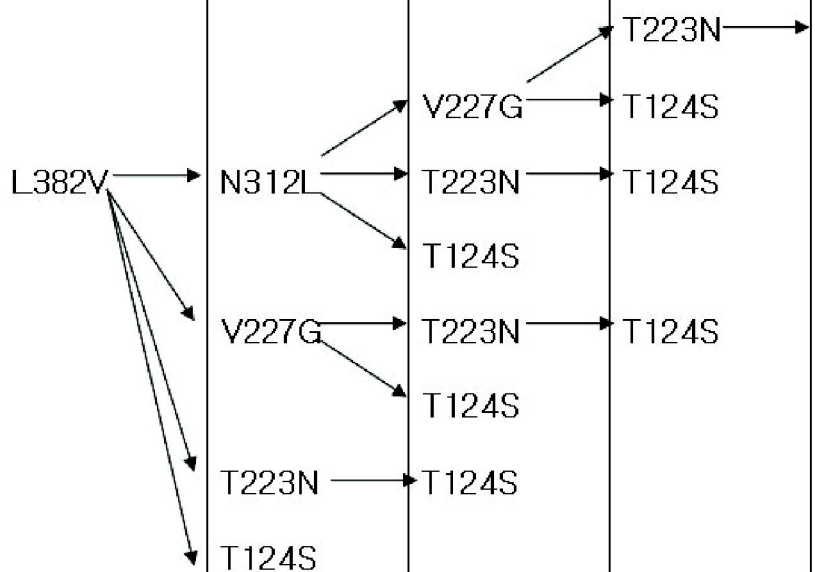
Type of the Mutant	Double Mutant	Triple Mutant	Quadruple Mutant	Quintuple Mutant
No. of Combinations	4	6	4	1

Figure 5